Diffusion, fragmentation, and coagulation processes: Analytical and numerical results

Poul Olesen,* Jesper Ferkinghoff-Borg,† Mogens H. Jensen,‡ and Joachim Mathiesen§
The Niels Bohr Institute, Blegdamsvej 17, DK-2100 Copenhagen, Denmark
(Received 19 November 2004; published 9 September 2005)

We formulate dynamical rate equations for physical processes driven by a combination of diffusive growth, size fragmentation, and fragment coagulation. Initially, we consider processes where coagulation is absent. In this case we solve the rate equation exactly leading to size distributions of Bessel type which fall off as $\exp(-x^{3/2})$ for large x values. Moreover, we provide explicit formulas for the expansion coefficients in terms of Airy functions. Introducing the coagulation term, the full nonlinear model is mapped exactly onto a Riccati equation that enables us to derive various asymptotic solutions for the distribution function. In particular, we find a standard exponential decay $\exp(-x)$ for large x and observe a crossover from the Bessel function for intermediate values of x. These findings are checked by numerical simulations, and we find perfect agreement between the theoretical predictions and numerical results.

DOI: 10.1103/PhysRevE.72.031103 PACS number(s): 82.30.Lp, 68.35.Fx, 68.43.Jk

I. INTRODUCTION

Since the pioneering work of von Smoluchowski [1,2] dating back to the beginning of the last century, the literature on coagulation and fragmentation processes has grown considerably. von Smoluchowski's original coagulation equation [1,2] provides a mean-field description of clusters that coalesce by binary collisions with a constant rate. Scaling theory and exactly solvable models in the kinetics of irreversible aggregation have recently been reviewed in [3].

Fragmentation and coagulation were first considered as combined processes in [4], and mean-field-type coagulation-fragmentation models have subsequently been used in a diverse range of applications, including polymer kinetics [5], aerosols [6], cluster formation in astrophysics [7], and animal grouping in biology [8,9]. We refer to [10,11] (and references therein) for a survey of the progress in the study of coagulation-fragmentation process.

Recently, we have suggested a mean-field model describing the dynamics of coherent structures, like ice crystals and structural elements of biomolecules, which grow or shrink randomly due to the diffusive motion of their boundaries and are subject to occasional fragmentation [12,13]. In this paper, we present an extension of the model to account for coagulation processes as well. The extension can be considered as a generalization of the von Smoluchowski coagulation-fragmentation equation to include processes where size diffusion is important. We emphasize that our approach differs from the approach in, e.g., [14], where the clusters represent particles immersed in a gas or liquid type of medium and the diffusive term added to the coagulation-fragmentation equation represents the random movement of the center of mass of each cluster. In contradistinction, we are focusing on systems where diffusion operates in the size space rather than in real space.

Diffusive growth processes are encountered in numerous physical systems. For instance, the process behind grain growth in ice or metallurgical systems can effectively be described as a size diffusive process, where the diffusion constant depends on the surface tension and the mobility of the grain boundaries (in the absence of extrinsic drag forces resulting from, e.g., impurities in the material); see, e.g., [12,13,15–18]. Size diffusion also appears in natural conjunction with convective growth in systems where the clusters in concern are coupled to a medium mediating the addition or subtraction of monomeric units. Crystal growth dynamics by reversible solute addition has, for instance, been considered in [19] in the limit of no coagulation and fragmentation. The combined process of fragmentation, size diffusion, and convection has been studied in [20,21] to describe the abrupt transitions from the growing to the shrinking state of microtubules. In both cases, the effective convective and diffusive growth can be directly related to the rate equations for monomer attachment and detachment from and to the medium (see, e.g., [19]). Finally, structural transitions in polypeptide systems [22] can be modeled by a continuous master equation with a size diffusive term representing the random fluctuations of the ordered-disordered interface [12].

Although we are not aware of previous work where diffusive growth appears in conjunction with cluster coagulation, we believe—in light of the examples given above—that such an extension of von Smoluchowski's original fragmentation-coagulation model is natural and should find application in several physical systems. Our aim in this paper is therefore to elucidate the effect of size diffusion in simple models of coagulation-fragmentation processes.

To proceed, let $N(x,t)$ denote the number of clusters of size x at time t. The general form of the coagulation-fragmentation model then reads [10]

$$\partial_t N(x,t) = [\partial_t N]_{\text{coag}} + [\partial_t N]_{\text{frag}}, \tag{1}$$

where

*Electronic address: polesen@nbi.dk
†Electronic address: borg@nbi.dk
‡Electronic address: mhjensen@nbi.dk
§Electronic address: mathies@nbi.dk

$$[\partial_t N]_{\text{coag}} = \frac{1}{2}\int_0^x K(x-x',x')N(t,x-x')N(t,x')dx' - N(t,x)\int_0^\infty K(x,x')N(t,x')dx'$$

and

$$[\partial_t N]_{\text{frag}} = -N(x,t)\int_0^x F(x-x',x')dx' + 2\int_0^\infty F(x,x')N(x+x',t)dx'.$$

The microscopic details of a given physical model are embedded in the kernels $K(x,x') \geq 0$ and $F(x,x') \geq 0$ (symmetric in x and x') which represent, respectively, the rate of the coagulation of two clusters of sizes x and x' into one cluster of size $x+x'$ and the rate of fragmentation of a cluster of size $x+x'$ into two clusters of size x and x'. The possible exchange of monomeric units with an external medium can be modeled by adding a convective and diffusive term to the equation which then reads

$$\partial_t N(x,t) = -v(x)\partial_x N(x,t) + D(x)\partial_x^2 N(x,t) + [\partial_t N]_{\text{coag}} + [\partial_t N]_{\text{frag}}. \quad (2)$$

Here, the first term describes the average drift of the cluster sizes due to monomeric exchange with the medium and the second term represents the random fluctuations superimposed on this drift (size diffusion). In the following we will examine analytical and numerical aspects of this equation with the simple choice of size-independent parameters $D(x)=D$, $F(x,x')=f$, and $K(x,x')=\beta$ and setting $v=0$. The model presented in [12,13] for the dynamics of ice crystals and structural building blocks in biomolecules corresponds to the case of no coagulation $\beta=0$. In these cases the systems are considered closed, so the $v=0$ condition follows from excluding any external driving. When the system is in a solution allowing for the solute-solvent exchange of monomeric units (as in, e.g., [19–21]) the $v=0$ condition corresponds to a situation where the solute (clusters) are in thermodynamical equilibrium with the solvent. The existence of steady states in the model with no coagulation has recently been identified for a wider class of fragmentation kernels [23], where connections to the pure fragmentation equation [24] and the so-called "shattering" transition [25] related to the formation of dust particles are further discussed. In the absence of diffusion, the model has been applied to the kinetics of reacting polymers in [26,27], where the uniqueness of solutions and convergence to equilibrium in the limit $t \to \infty$ have been proved. As will be demonstrated, the inclusion of a diffusion term in the equation may lead to solutions radically different from the ones found in [26,27].

Our paper is organized as follows. In Sec. II, we derive the exact solution to the model in the case of no coagulation ($D>0, f>0, \beta=0$). Sections III and IV are devoted to a discussion of the expansion coefficients entering this solution. In particular, we give an explicit formula for the coefficients in terms of a orthogonal set of Airy functions and discuss their asymptotic behavior. A moment analysis of the solution in the large-time limit is carried out in Sec. V. In Sec. VI, we focus on the full diffusion-coagulation-fragmentation model. It is shown that the equation can be mapped to a Riccati equation, and we discuss its solutions in the case of no coagulation ($\beta=0$, Sec. VII) and no diffusion ($D=0$, Sec. VIII). Here, the solution to the diffusion-fragmentation model found in Secs. II–V becomes useful to elucidate the structure of the solutions to the Riccati equation. In Sec. IX we return to the full diffusion-fragmentation-coagulation model. We demonstrate that the equation possesses a transition point for the coagulation term, where the distribution crosses over from the Bessel behavior found in the pure fragmentation-diffusion case to an exponential. In the final section, we discuss two numerical implementations of the model.

II. SOLUTION TO THE FRAGMENTATION-DIFFUSION EQUATION

In the following three sections, we expand on the results of a recent Letter [12] on the diffusion-fragmentation equation. In particular, we shall carefully study the structure of the analytical solution of the diffusion-fragmentation equation. We shall derive orthogonality relations of the functions entering the solution and find the corresponding expansion coefficients. The general equation we wish to solve has the form

$$\partial_t N(x,t) = D\partial_x^2 N(x,t) - fxN(x,t) + 2f\int_x^\infty N(x',t)dx',$$

which is a particular case of Eq. (2) with size-independent diffusion and fragmentation terms and with no coagulation ($\beta=0$). Below we shall consider the boundary conditions $N(0,t)=0$ and $N(x,t)\to 0$ for $x\to\infty$ for all times t, including the initial condition at $t=0$.

We rescale time and the cluster size

$$x \to x/x_0 \quad \text{and} \quad t \to t/(fx_0)^{-1},$$

where $x_0=(D/f)^{1/3}$. A subsequent differentiation with respect to x leads to the equation

$$\partial_t\partial_x N(x,t) = \partial_x^3 N(x,t) - 3N(x,t) - x\partial_x N(x,t). \quad (3)$$

It is fairly easy to solve Eq. (3) by separation of variables. Taking $N(x,t)=T(t)X(x)$ we have

$$\dot{T}(t) = \lambda T(t), \quad X'''(x) - 3X(x) - xX'(x) = \lambda X'(x), \quad (4)$$

where λ is a separation constant. We shall simplify the notation by shifting the variable x such that the separation constant gets included, $x\to x-\lambda$. The equation for X can be solved [with the boundary condition $X(x)\to 0$ for $x\to\infty$] by means of a Fourier transform, with the result

$$X(x) = \frac{1}{2}\int_{-\infty}^\infty dk\ k^2 e^{ikx+ik^3/3} \equiv B(x). \quad (5)$$

Although x is positive, we need to consider $X(x)$ for negative values of x in Eq. (8). By analytical continuation the function

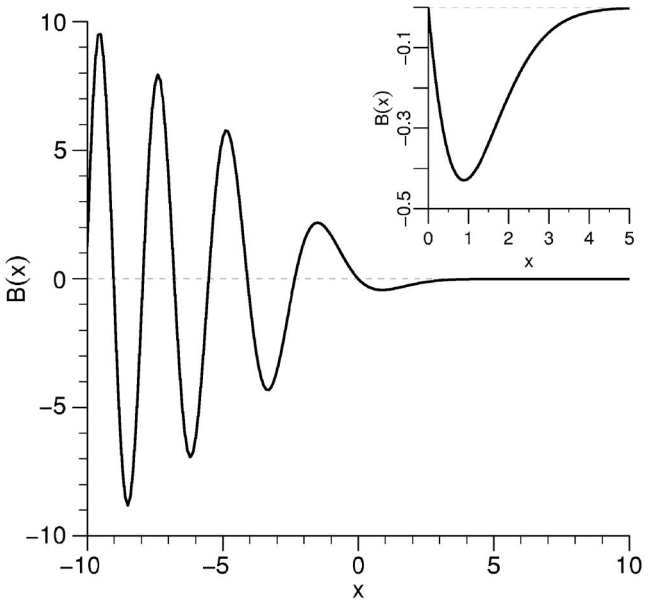

FIG. 1. The function $B(x)$ (x is dimensionless) and its intersections with $y=0$. Note that all intersections appears for $x<0$ only. Inset: a close-up of the function for positive x.

$X(x)$ is well defined for $x<0$. The function B is related to the Airy integral

$$A(x) \equiv \frac{1}{2}\int_{-\infty}^{\infty} dk\ e^{ikx+ik^3/3} = \int_0^{\infty} dk\ \cos\left(kx+\frac{k^3}{3}\right), \quad (6)$$

which has been discussed, e.g., in Ref. [28]; see in particular pp. 188–190. In the panels of Fig. 1 we show $B(x)$ for positive and negative values of x, respectively.

By differentiating $A(x)$ twice we get

$$B(x) = -\partial_x^2 A(x). \quad (7)$$

Collecting the results obtained above and inserting once again the separation constant, the solution of Eq. (3) can now be written

$$N(x,t) = \sum_n C_n e^{\lambda_n t} B(x+\lambda_n). \quad (8)$$

In case the eigenvalues λ_n are in a continuous range the sum should be replaced by an integral. We shall here impose an absorbing boundary conditions for small clusters, which implies that the probability of clusters with zero size vanishes at all times—i.e.,

$$N(0,t) = 0. \quad (9)$$

We implement this condition by requiring $B(\lambda_n)=0$. Thus the eigenvalues must be zeros of the function $B(x)$.

To find possible zeros of $B(x)$ we need some properties of the functions $A(x)$ and $B(x)$. It turns out that $A(x)$ can be expressed in terms of Bessel functions [28] by use of a deformation of the contour in Eq. (6), with the result

$$A(x) = \sqrt{\frac{x}{3}} K_{1/3}\left(\frac{2x^{3/2}}{3}\right) \quad \text{for} \quad x>0$$

$$= \frac{\pi}{3}\sqrt{|x|}\left[J_{1/3}\left(\frac{2|x|^{3/2}}{3}\right) + J_{-1/3}\left(\frac{2|x|^{3/2}}{3}\right)\right] \quad \text{for} \quad x<0. \quad (10)$$

The absolute signs in the last line should be noticed. The function $A(x)$ is positive for $x>0$ and oscillates for $x<0$, where it has an infinite number of zeros.

We can now differentiate $A(x)$, and using well-known functional relations[1] for the Bessel functions [28,29], one obtains the result

$$A'(x) = -\frac{x}{\sqrt{3}} K_{2/3}\left(\frac{2x^{3/2}}{3}\right) \quad \text{for} \quad x>0$$

$$= \frac{\pi}{3} x\left[J_{-2/3}\left(\frac{2|x|^{3/2}}{3}\right) - J_{2/3}\left(\frac{2|x|^{3/2}}{3}\right)\right] \quad \text{for} \quad x<0. \quad (11)$$

Performing another differentiation gives

$$A''(x) = x\sqrt{\frac{x}{3}} K_{1/3}\left(\frac{2x^{3/2}}{3}\right) \quad \text{for} \quad x>0$$

$$= \frac{\pi}{3} x\sqrt{-x}\left[J_{1/3}\left(\frac{2|x|^{3/2}}{3}\right) + J_{-1/3}\left(\frac{2|x|^{3/2}}{3}\right)\right] \quad \text{for} \quad x<0. \quad (12)$$

Comparison with Eq. (10) shows that $A(x)$ satisfies the simple second-order differential equation found by Stokes [28],

$$\partial_x^2 A(x) = xA(x), \quad (13)$$

which will play a crucial role in the following. Comparing this equation to Eq. (7) we see the remarkably simple relation between $B(x)$ and $A(x)$,

$$B(x) = -xA(x). \quad (14)$$

From well-known properties of the Bessel functions K and J we see that the function $A(x)$ has zeros for $x=\lambda_n<0$ with

$$J_{1/3}\left(\frac{2|\lambda_n|^{3/2}}{3}\right) + J_{-1/3}\left(\frac{2|\lambda_n|^{3/2}}{3}\right) = 0. \quad (15)$$

These zeros can be computed easily numerically. The first few are given approximately by

$$\lambda_1 = -2.338,\ \lambda_2 = -4.088,\ \lambda_3 = -5.521,$$

[1]We use $zJ'_\nu(z)+\nu J_\nu(z)=zJ_{\nu-1}(z)$ and $zJ'_\nu(z)-\nu J_\nu(z)=-zJ_{\nu+1}(z)$ and the relations for the K functions, $K'_\nu(z)=-(\nu/z)K_\nu(z)-K_{\nu-1}(z)$ and $K_\nu(z)=K_{-\nu}(z)$.

$$\lambda_4 = -6.787,\ \lambda_5 = -7.945,\ \lambda_6 = -9.023. \tag{16}$$

It should be mentioned that from the asymptotic form of the Bessel functions the zeros are approximately given by

$$\lambda_n \approx -\left[\frac{3\pi}{2}\left(n+\frac{3}{4}\right)\right]^{2/3}. \tag{17}$$

This expression is valid for large n. However, the expression provides a surprisingly accurate estimate of λ_{n+1} even for small n's. For example, for $n=0$ one finds that Eq. (17) gives -2.32, as compared to the numerically obtained more accurate value $\lambda_1=-2.338$. For $n=3$ one obtains ≈ -6.785 to be compared to the more accurate $\lambda_4=-6.787$.

We now return to the boundary condition (9) which is to be implemented on the solution (8). This requires

$$N(0,t) = \sum_{n=0}^{\infty} C_n B(\lambda_n) = 0. \tag{18}$$

Taking into account Eq. (14) giving the relation between $A(x)$ and $B(x)$ as well as expression (10) for $A(x)$, we thus see that the λ_n's are discrete (since there are only discrete zeros in the Bessel functions); they must be negative and must also satisfy Eq. (15). However, even though $A(0)\neq 0$, it follows from Eq. (14) that $B(0)=0$. Therefore the sum in Eq. (18) includes $n=0$ with $\lambda_0=0$.

The solution to Eq. (3) is thus

$$N(x,t) = C_0 B(x) + \sum_{n=1}^{\infty} C_n e^{\lambda_n t} B(x+\lambda_n). \tag{19}$$

Here we separated the first term explicitly in order to emphasize that it is time independent. Since the λ_n's are negative for $n\neq 0$, it follows that after a sufficiently long time the first term dominates,

$$N(x,t) \to C_0 B(x) \quad \text{for} \quad t\to\infty. \tag{20}$$

Note that $C_0<0$. In order to use Eq. (19) we need to determine the constants C_n. This problem will be discussed in the next section.

III. ORTHOGONALITY

The solution (19) is incomplete as it stands since we need to determine the expansion coefficients. This problem is related to orthogonality of the functions entering this solution. It turns out that the $B(x+\lambda_n)$'s are not orthogonal,[2] which is connected to the fact that the B function satisfies the third-order differential equation (3). However, we shall now use the fact that $A(x)$ satisfies the second-order differential equation (13), so we can use standard orthogonality considerations as far as $A(x)$ is concerned. Therefore instead of $N(x,t)$ we consider the function

$$M(x,t) = \sum_{n=0}^{\infty} C_n e^{\lambda_n t} A(x+\lambda_n), \tag{21}$$

where the constants C_n are the same as in Eq. (8). The connection between $N(x,t)$ and $M(x,t)$ is given by

$$\partial_x^2 M(x,t) = -N(x,t) \tag{22}$$

as a consequence of Eq. (7).

We can now show that the functions $A(x+\lambda_n)$ form an orthogonal set of functions for $\lambda_n\neq 0$. From Eq. (13) we have

$$A''(x+\lambda_n) = (x+\lambda_n)A(x+\lambda_n). \tag{23}$$

This second-order equation allows us to use standard methods, in contrast to the original third-order equation for $N(x,t)$. Thus we obtain

$$\int_0^{\infty} dx[A(x+\lambda_m)A''(x+\lambda_n) - A(x+\lambda_n)A''(x+\lambda_m)]$$
$$= (\lambda_n-\lambda_m)\int_0^{\infty} dx A(x+\lambda_n)A(x+\lambda_m). \tag{24}$$

Following standard procedures we now shift the two differentiations in the first term in the integrand on the left-hand side by two partial differentiations. In this way the first term cancels the second, except for contributions from the boundaries. For $x=\infty$ there are no contributions, since the Bessel function vanishes exponentially. Taking into account the contributions from the lower limit $x=0$ we have

$$(\lambda_n-\lambda_m)\int_0^{\infty} dx A(x+\lambda_n)A(x+\lambda_m)$$
$$= -A(\lambda_m)A'(\lambda_n) + A'(\lambda_m)A(\lambda_n). \tag{25}$$

However, since λ_n are the zeros of the function A for $n\neq 0$, we have $A(\lambda_m)=A(\lambda_n)=0$. It is important to notice that neither $A(0)$ nor $A'(0)$ vanishes. For $n\neq 0$ the quantity on the right-hand side of Eq. (25) vanishes, and hence

$$(\lambda_n-\lambda_m)\int_0^{\infty} dx A(x+\lambda_n)A(x+\lambda_m) = 0 \quad \text{for } n \text{ and } m \neq 0. \tag{26}$$

Thus the set $\{A(x+\lambda_n)\}$ consists of orthogonal functions, except for $\lambda_0=0$. It then follows that the expansion coefficients in Eq. (21) are determined through the equation[3] [12,13]

$$C_m = \frac{1}{I_m}\left[\int_0^{\infty} dx\, M(x,0)A(x+\lambda_m) - C_0\int_0^{\in} fty dx A(x+\lambda_m)A(x)\right], \quad m\neq 0, \tag{27}$$

where

[2] This can easily be seen in examples by doing the relevant integrals numerically. Thus, for example, the integral $\int_0^{\infty} dx B(x-2.338)B(x-4.088)$ has the nonvanishing value -9.102.

[3] If the initial data are taken to be given at time t_0 instead of $t=0$, C_m should be replaced by $C_m e^{\lambda_n t_0}$ and $M(x,0)$ by $M(x,t_0)$ in Eq. (27). Similarly, in the solution $e^{\lambda_n t}$ is replaced by $e^{\lambda_n(t-t_0)}$

$$I_m = \int_0^\infty dx\, A(x+\lambda_m)^2. \tag{28}$$

In the next section we shall show the I_m can be expressed in terms of $A'(\lambda_n)$, which in turn can be expressed in terms of Bessel functions [28].

Taking $\lambda_m=0$ we obtain, from Eq. (25),

$$\int_0^\infty dx A(x+\lambda_n)A(x) = -\frac{A(0)A'(\lambda_n)}{\lambda_n}, \tag{29}$$

which we shall use in the next section.

In expression (27) for C_n the function $M(x,0)$ enters. However, the relevant initial function is $N(x,0)$. We can re-express C_m in terms of $N(x,0)$ by solving Eq. (22) for M in terms of N. Noticing that the Greens function in one dimension is $\theta(x)x$, we easily obtain, from Eq. (22),

$$M(x,0) = \alpha + \beta x - \int_0^x dx'(x-x')N(x',0), \tag{30}$$

where α and β are integration constants. It follows from the definition, Eq. (21), of M that $M(0,0)=C_0A(0)$, since $A(\lambda_n)=0$ for $n\neq 0$. Thus $\alpha=C_0A(0)$.

To find the constant β consider

$$\partial_x M(x,0)|_{x=0} = \beta = \sum_{n=0}^\infty C_n A'(\lambda_n). \tag{31}$$

Now from the solution (8) we have, by use of Eq. (7),

$$\int_0^\infty dx\, N(x,0) = \sum_{n=0}^\infty C_n \int_0^\infty dx B(x+\lambda_n)$$
$$= -\sum_{n=0}^\infty C_n \int_0^\infty dx \partial_x^2 A(x+\lambda_n) = \sum_0^\infty C_n A'(\lambda_n). \tag{32}$$

Therefore,

$$\beta = \int_0^\infty dx\, N(x,0). \tag{33}$$

We now insert these results into Eq. (30) which becomes

$$M(x,0) = -\int_0^x dx\,(x-x')N(x',0)$$
$$+ x\int_0^\infty dx'\, N(x',0) + C_0A(0). \tag{34}$$

To proceed we need also to determine C_0. We have, by use of Eqs. (7) and (8),

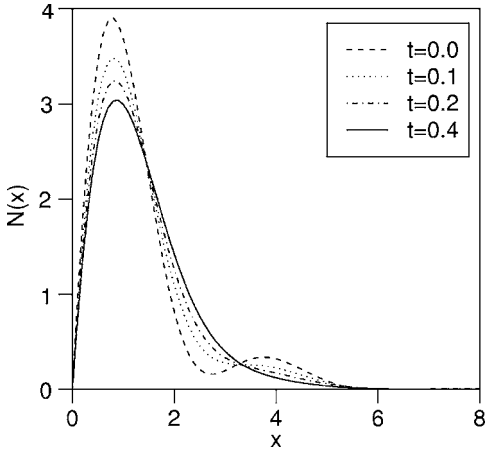

FIG. 2. An example showing the time development of $N(x,t)$ (x and t are dimensionless) with a secondary peak, which ultimately disappears. The specific values of the expansion parameters C_n are $(C_0,C_1,C_2,\ldots)=(-7,-0.2,-0.2,0.05,-0.035)$.

$$\int_0^\infty dx\, xN(x,0) = \sum_{n=0}^\infty C_n \int_0^\infty dx\, xB(x+\lambda_n)$$
$$= -\sum_{n=0}^\infty C_n \int_0^\infty dx x \partial_x^2 A(x+\lambda_n) = -C_0A(0), \tag{35}$$

so

$$C_0 = -\frac{1}{A(0)}\int_0^\infty dx\, xN(x,0), \quad A(0) = \frac{\pi}{3^{2/3}\Gamma(2/3)}. \tag{36}$$

Thus C_0 is determined in terms of the initial data for N.

We can now insert the result (36) into Eq. (34),

$$M(x,0) = \int_x^\infty dx'(x-x')N(x',0). \tag{37}$$

This finally gives an expression for the expansion coefficients in terms of the initial value for N,

$$C_m = \frac{1}{I_m}\int_0^\infty dx\, A(x+\lambda_m)\left[\int_x^\infty dx'(x-x')N(x',0) - C_0A(x)\right], \tag{38}$$

where we inserted the solution (37) of M in terms of N in expression (27) for C_m. In Fig. 2 we show an example of the evolution of $N(x,t)$ with the interesting feature of the presence of a secondary peak. Interchanging the x and x' integrations this expression can be rewritten in a form which is more suitable for insertions of data for $N(x,0)$: namely,

$$C_m = \frac{1}{I_m}\left[\int_0^\infty dx\, N(x,0)\int_0^x dx'(x'-x)A(x'+\lambda_m) - C_0\int_0^\infty dx\, A(x+\lambda_m)A(x)\right]$$
$$= \frac{1}{I_m}\int_0^\infty dx\, N(x,0)\left\{A'(x+\lambda_m) - A'(\lambda_m) - (x+\lambda_m)\int_0^x dx'\, A(x'+\lambda_m) + \frac{x}{A(0)}\int_0^\infty dx'\, A(x'+\lambda_m)A(x')\right\}. \quad (39)$$

To obtain the last form we used Eq. (7) and inserted C_0. Thus, to sum up the solution of Eq. (54) is given by Eq. (74), with B given by Eqs. (10) and (14), and with C_n given by Eq. (39). It should be emphasized that in Eq. (39) the initial function $N(x,0)$ enters only in the first integral, whereas the other integrals involving the function A can be determined numerically to any desired accuracy.

IV. EXPANSION COEFFICIENTS

In this section we shall examine the expansion coefficients C_m given by Eqs. (38) and (39). We start by considering the normalization integrals I_m defined by Eq. (28). The differential equation (13) for $A(x)$, $A''=xA$, can be rewritten as $2A'A''-2xAA'-A^2=-A^2$—i.e.,

$$\frac{d}{dx}[A'(x)^2 - xA(x)^2] = -A(x)^2, \quad (40)$$

so that the normalization integral becomes

$$I_m = \int_{\lambda_m}^\infty dx A(x)^2 = A'(\lambda_m)^2, \quad (41)$$

where we used that $A(\lambda_m)=0$.

We can now express I_m in terms of Bessel functions by differentiating $A(x)$ given in Eq. (10) and using standard functional relations for the relevant Bessel functions [28,29]. Using $A'(x)$ already evaluated in Eq. (11) we have

$$I_m = \frac{\pi^2}{9}\lambda_m^2[J_{-2/3}(2|\lambda_m|^{3/2}/3) - J_{2/3}(2|\lambda_m|^{3/2}/3)]^2. \quad (42)$$

If we use the well-known asymptotic expansions of the Bessel functions as well as the asymptotic eigenvalue (17), it is easy to see that Eq. (42) becomes

$$I_m \approx \pi^{4/3}\left(\frac{3}{2}\right)^{1/3}\left(m+\frac{3}{4}\right)^{1/3}, \quad m\to\infty. \quad (43)$$

We have compared Eq. (43) with the exact expression (42) even for small m. We find that for $m=0$ the analytic expression (42) gives 4.852 85, whereas the approximate result (43) gives 4.785. For $m=4$ the corresponding numbers are 8.857 37 and 8.8538. For $m\geqslant 5$ one gets the first two decimals right.

The first expression (39) can now be simplified by use of Eq. (29),

$$C_m = \frac{1}{A'(\lambda_m)^2}\int_0^\infty dx N(x,0)\int_0^x dx'(x'-x)A(x'+\lambda_m) - \frac{1}{\lambda_m A'(\lambda_m)}\int_0^\infty dx x N(x,0), \quad m\neq 0. \quad (44)$$

From the asymptotic statements (17) and (43) we see that the last term on the right-hand side of Eq. (44) behaves like $m^{-5/6}$. However, in the expansion for M this is to be multiplied by the oscillating function $A(x+\lambda_n)$. In any case it should be noticed that if $t\neq 0$, there is no convergence problem because the exponential damping factors $e^{\lambda_m t}$ give rapid convergence. Convergence problems in the form of very slow convergence may arise at the initial time, where the expansion coefficients are determined in terms of the initial data.

V. MEAN VALUES

We shall now compute the mean values $\bar{x}$ and $\overline{x^2}$, which turn out to be given by rather simple expressions for large times. We have

$$\bar{x} = \int_0^\infty dx\, xN(x,t)/\int_0^\infty dx\, N(x,t),$$
$$\overline{x^2} = \int_0^\infty dx\, x^2 N(x,t)/\int_0^\infty dx\, N(x,t). \quad (45)$$

By the methods already used in Eqs. (32) and (35) we obtain

$$\bar{x} = -A(0)/\left(A'(0) + (1/C_0)\sum_{n=1}^\infty C_n e^{\lambda_n t}A'(\lambda_n)\right). \quad (46)$$

We also have by use of Eq. (7) and two partial integrations

$$\int_0^\infty dx\, x^2 N(x,t) = -2\sum_{n=0}^\infty C_n e^{\lambda_n t}\int_0^\infty dx\, A(x+\lambda_n). \quad (47)$$

In the limit $t\to\infty$ we obtain the simple results

$$\bar{x} \to \frac{3^{2/3}\Gamma(4/3)}{\Gamma(2/3)} \approx 1.3717, \quad (48)$$

as well as

$$\overline{x^2} \approx 2.5758. \quad (49)$$

Here we used that $\int_0^\infty dx\, A(x) \approx 1.0472$. The relative dispersion therefore becomes

$$\frac{D^2}{\bar{x}^2} \equiv \frac{\overline{x^2-\bar{x}^2}}{\bar{x}^2} \approx 0.36897 \quad (50)$$

for $t\to\infty$. The dispersion is therefore smaller than $\bar{x}$, $D \approx 0.607\,43\bar{x}$.

VI. TRANSFORMATION OF THE MODEL WITH FINITE COAGULATION TO A RICCATI EQUATION

In this section we shall discuss the model, Eq. (2), with constant diffusion and finite size-independent fragmentation and coagulation kernels, $f>0$ and $\beta>0$. The basic equation for the steady-state solution is thus [30]

$$D\partial_x^2 N(x) - fxN(x) + 2f\int_x^\infty dx' N(x') + \beta/2\int_0^x dx' N(x')N(x-x') - 2\tilde{\beta}N(x) = 0, \quad (51)$$

where

$$\tilde{\beta} = \beta/2\int_0^\infty dx N(x). \quad (52)$$

By integrating Eq. (51) we easily get

$$\frac{D\beta}{f^2}N'(0) = \frac{\beta}{f}\int_0^\infty dx\, xN(x) - 2b^2 \geqslant 0, \quad (53)$$

where $b=\tilde{\beta}/f$ represents a new length scale compared to the one given by the diffusion to fragmentation ratio, $x_0=(D/f)^{1/3}$, as previously introduced.

Equation (51) is an integro-differential equation. In general we would like to solve this equation with the boundary conditions that $N(0)=0$ and $N(x)\to 0$ for $x\to\infty$. Furthermore, we need of course also to invoke the condition that $N(x)$ be positive. This is not automatically guaranteed from Eq. (51). We shall see that if diffusion is absent, it is not possible to achieve $N(0)=0$. The main result of this section is that in Fourier space the integro-differential equation (51) can be mapped onto a Riccati equation or, alternatively, a linear second-order differential equation. If we can achieve $N(0)=0$, we need $N'(0)\geqslant 0$ from positivity of $N(x)$, and hence the right-hand side of Eq. (53) must be positive. Since Eq. (53) is a consequence of Eq. (51), a solution for the function $N(x)$ should satisfy Eq. (53) automatically.

In the presence of diffusion, we can make Eq. (51) dimensionless by rescaling the cluster size $x\to x/x_0$ as in Sec. II:

$$\partial_x^2 N(x) - xN(x) + 2\int_x^\infty dx' N(x') + \frac{\beta}{2fx_0}\int_0^x dx' N(x')N(x-x') - \frac{2b}{x_0}N(x) = 0. \quad (54)$$

We now take the Fourier transform

$$N(x) = \int_{-\infty+i\epsilon}^{\infty+i\epsilon} d\omega\, e^{i\omega x}\tilde{N}(\omega) = e^{-\epsilon x}\int_{-\infty}^{\infty} d\omega\, e^{i\omega x}\tilde{N}(\omega), \quad (55)$$

where the convergence factor is needed in the following. Alternatively we can consider the contour to be shifted slightly to the upper half plane. We assume that the function $\tilde{N}(\omega)$ is continuous as the real axis is approached.

We can now translate Eq. (54) to Fourier space. For example, we use

$$\int_x^\infty dx' N(x') = \int_{-\infty}^{\infty} d\omega\, \tilde{N}(\omega)\int_x^\infty e^{i\omega x'-\epsilon x} = i\int_{-\infty+i\epsilon}^{\infty+i\epsilon} d\omega \frac{\tilde{N}(\omega)}{\omega}e^{i\omega x}. \quad (56)$$

Here the convergence factor is of course important. Putting everything together we obtain, from Eq. (54),

$$\int_{-\infty+i\epsilon}^{\infty+i\epsilon} d\omega\, e^{i\omega x}\mathcal{O}(\omega)\tilde{N}(\omega) = \frac{\beta}{2fx_0}\iint_{-\infty+i\epsilon}^{\infty+i\epsilon} d\omega d\omega' \frac{\tilde{N}(\omega)\tilde{N}(\omega')}{\omega-\omega'}(e^{i\omega x}-e^{i\omega' x}), \quad (57)$$

where the operator $\mathcal{O}$ is given by

$$\mathcal{O}(\omega) = -\omega^2 + \frac{2i}{\omega} - \frac{2b}{x_0} - i\frac{d}{d\omega}. \quad (58)$$

From this we obtain by an integration over x from 0 to ∞ with the weight factor $\exp(-i\tau x)$,

$$i\int_{-\infty+i\epsilon}^{\infty+i\epsilon} d\omega \frac{\mathcal{O}(\omega)\tilde{N}(\omega)}{\omega-\tau} = \frac{\beta}{2fx_0}F(\tau)^2, \quad (59)$$

where F is the Hilbert transform:

$$F(\tau) = \int_{-\infty+i\epsilon}^{\infty+i\epsilon} d\omega \frac{\tilde{N}(\omega)}{\tau-\omega}. \quad (60)$$

Equation (59) can be reformulated as an equation for F. To do this, we rewrite $\omega^2=(\omega^2-\tau^2)+\tau^2$ to obtain[4]

$$\int d\omega \frac{\omega^2\tilde{N}(\omega)}{\omega-\tau} = \int d\omega(\omega+\tau)\tilde{N}(\omega) + \tau^2 F(\tau) = -iN'(0) + \tau N(0) + \tau^2 F(\tau). \quad (61)$$

We want to solve the problem with the boundary condition $N(0)=0$, so in the following the linear term on the right-hand side will be left out. We also have

$$\int d\omega \frac{\tilde{N}(\omega)}{\omega(\omega-\tau)} = \frac{i\tilde{\beta}}{\beta\tau} + \frac{1}{\tau}F(\tau). \quad (62)$$

Collecting these results Eq. (59) becomes

[4]In order to simplify the notation we leave out the limits on the ω integration, always assuming that this integration goes from $-\infty+i\epsilon$ to $\infty+i\epsilon$ in the following.

$$\frac{\beta}{2fx_0}F(\tau)^2 = -\frac{dF(\tau)}{d\tau} + \left(\frac{2}{\tau} + i\tau^2 + \frac{2ib}{x_0}\right)F(\tau) - N'(0) - 2i\frac{\tilde{\beta}}{\beta\tau}. \tag{63}$$

This is a standard equation of the Riccati type. It should be noticed that if there is no diffusion the Riccati equation simplifies to

$$\frac{\beta}{2f}F(\tau)^2 = -\frac{dF(\tau)}{d\tau} + \left(\frac{2}{\tau} + 2ib\right)F(\tau) - 2i\frac{\tilde{\beta}}{\beta\tau} \quad \text{(no diffusion)}, \tag{64}$$

where τ now has the dimension of length^{-1}.

It is well known that a Riccati equation can be transformed to a linear second-order differential equation by the substitution

$$\frac{\beta}{2fx_0}F(\tau) = \frac{d}{d\tau}\ln u(\tau), \tag{65}$$

where u satisfies

$$u''(\tau) - \left(\frac{2}{\tau} + i\tau^2 + 2i\frac{b}{x_0}\right)u'(\tau) + \left(\frac{\beta}{2fx_0}N'(0) + \frac{2ib}{x_0\tau}\right)u(\tau) = 0. \tag{66}$$

The original Fourier transform (55) was given in terms of the function $\tilde{N}$, which in turn is related to the function F by the Hilbert transform (60). However, it is well known that the Fourier transform of a Hilbert transform has a remarkably simple property, which in our case (since $x>0$) leads to

$$N(x) = \frac{1}{2\pi i}\int_{-\infty}^{\infty} d\tau e^{i\tau x}F(\tau). \tag{67}$$

This equation can be derived by noticing that since the ω integration is shifted to slightly above the real axis, we have

$$F(\tau) = F_P(\tau) + i\pi\tilde{N}(\tau), \quad F_P(\tau) = P\int_{-\infty}^{\infty} d\omega\frac{\tilde{N}(\omega)}{\tau-\omega}, \tag{68}$$

where P means the principal value. Further we have

$$N(x) = \int d\omega\,\tilde{N}(\omega)e^{i\omega x} = \frac{1}{i\pi}\int d\omega\,\tilde{N}(\omega)e^{i\omega x}P\int_{-\infty}^{\infty} dy\frac{e^{iyx}}{y}$$

$$= \frac{1}{i\pi}\int d\tau e^{i\tau x}F_P(\tau), \tag{69}$$

where we used that, for $x>0$,

$$P\int_{-\infty}^{\infty} dy\frac{e^{iyx}}{y} = i\pi \tag{70}$$

and where we took $y=\tau-\omega$. Using Eq. (68) we obtain Eq. (67).

From Eq. (67) we see that the original integro-differential equation (54) is solved if we can solve the Riccati equation (63) or, alternatively, the linear second-order differential equation (66).

VII. CASE OF NO MERGING

Before we discuss the Riccati equation it is quite instructive to consider the case of no merging, $\beta=0$. In our previous work we have solved this problem in terms of the Airy function [12,13] with the result

$$N(x)_{\beta=0} = \text{const} \times \int_{-\infty}^{\infty} d\omega\,\omega^2 e^{i\omega^3/3+i\omega x}. \tag{71}$$

This function solves the equation

$$\mathcal{O}(\omega)\tilde{N}(\omega) = 0 \tag{72}$$

subject to the boundary condition that $N(x)\to 0$ for $x\to\infty$,

With the present method we obtain from Eq. (63), with $\beta=0$,

$$-\frac{dF(\tau)}{d\tau} + \left(\frac{2}{\tau} + i\tau^2\right)F(\tau) - N'(0) - 2i\frac{c}{\tau} = 0, \tag{73}$$

where the constant c is given by $c=\tilde{\beta}/\beta=\int_0^\infty dxN(x)$. The solution is given by

$$F(\tau) = \tau^2 e^{i\tau^3/3}\left[K - \int\frac{d\tau}{\tau^2}e^{-i\tau^3/3}\left(N'(0) + 2i\frac{c}{\tau}\right)\right]. \tag{74}$$

Here K is a constant of integration. Comparing to the correct result (71) by use of the Fourier transform (67) in terms of F, we see that the second term in the solution (74) apparently gives a deviation from Eq. (71).

The resolution of this paradox is that the last term in Eq. (74) does not give any contributions to the Fourier integral. This can be seen by noticing that the indefinite integral in Eq. (74) can be expressed in terms of the incomplete Γ function, and when multiplied by the prefactor $\tau^2 e^{i\tau^3/3}$ it is analytic in the upper half plane. When we plug the second term in Eq. (74) into the Fourier integral (67) we can close the integration by a large circle in the upper half plane. This circle contributes nothing, since the factor $\exp(i\tau x)$ gives an exponential damping on the circle and since the behavior of the second term (including the prefactor) in Eq. (74) is $-iN'(0)/\tau^2 + O(1/\tau^3)$ for large τ, as can be seen by a partial integration. This behavior does not compete with the exponential damping. Therefore,

$$-\tau^2 e^{i\tau^3/3}\int\frac{d\tau}{\tau^2}e^{-i\tau^3/3}\left(N'(0) + 2i\frac{c}{\tau}\right) \tag{75}$$

is a null function in the Fourier integral (67).

The moral of this story is that although the function $N(x)$ is given by the two integrals (55) and (67), this does not mean that the two functions $\tilde{N}$ and F are proportional. They can differ by a nontrivial null function. As the example given above shows, we must in general expect the occurrence of such nontrivial null functions.

Another point which should be mentioned is why the first term in the solution (74) cannot be treated like the second term: In the second term the factors $\exp(\pm i\tau^3/3)$ cancel out, as one can see by repeated partial integrations of the integral in the solution (74). For example, for small τ one has

$$\tau^2 e^{i\tau^3/3}\int \frac{d\tau}{\tau^3}e^{-i\tau^3/3} = -\frac{1}{2} - \frac{i}{2}\tau^2 e^{i\tau^3/3}\int d\tau\, e^{-i\tau^3/3}$$

$$= -\frac{1}{2} - \frac{i}{2}\tau^3 + \cdots . \tag{76}$$

A similar argument does not apply to the first factor in Eq. (74) which contains $\exp(i\tau^3/3)$ and does not give convergence on the large circle: This factor overwhelms the damping from $\exp(i\tau x)$. Actually the contour can only be be closed in the upper half plane by two straight lines in the directions $\pi/6$ and $5\pi/6$. The closed contour running along the real axis from $-\infty$ to $+\infty$, a part of a circle at infinity going from the angle 0 to $\pi/6$ (gives no contribution due to a damping factor $\exp[-|\omega|^3\sin(3\phi)]$, $0<\phi<\pi/6$), runs back to the origin along a straight line, moves to the left along a line making the angle $5\pi/6$, and is closed by a circle going towards the real axis (gives no contribution). On the straight lines the factor $\exp(i\tau^3/3)$ becomes strongly damped and behaves like $\exp(-|\tau|^3/3)$. Therefore the oscillating integral (71) can be replaced by the strongly damped integral

$$N(x)_{\beta=0} = \text{const} \times \int_0^\infty d\tau\, \tau^2 e^{-\tau^3/3 - \tau x \sin \pi/6}\sin(\tau x \cos \pi/6). \tag{77}$$

VIII. CASE OF NO DIFFUSION

We shall now consider the case without diffusion, where the Riccati equation simplified to Eq. (64) with the corresponding second-order equation

$$u''(\tau) - \left(\frac{2}{\tau} + 2ib\right)u'(\tau) + \frac{2ib}{\tau}u(\tau) = 0. \tag{78}$$

This equation can be solved in terms of Bessel functions,

$$u(\tau) = k\tau^{3/2}e^{ib\tau}[J_{-3/2}(-b\tau) + CN_{-3/2}(-b\tau)], \tag{79}$$

where k and C are constants. These Bessel functions can be expressed in terms of trigonometric functions,

$$J_{-3/2}(-b\tau) = \pm i\sqrt{\frac{2}{\pi\tau b}}\left(\sin(b\tau) + \frac{\cos(\tau b)}{b\tau}\right),$$

$$N_{-3/2}(-b\tau) = \pm i\sqrt{\frac{2}{\pi\tau b}}\left(\cos(b\tau) - \frac{\sin(\tau b)}{b\tau}\right). \tag{80}$$

For the function F we then get

$$F(\tau) = ib\frac{2f}{\beta}\frac{[1+b\tau(C-i)]\cos(b\tau) - [C - b\tau(1+iC)]\sin(b\tau)}{(1+Cb\tau)\cos(b\tau) + (b\tau - C)\sin(b\tau)}, \tag{81}$$

where C is a constant of integration. Since F is given by a Hilbert transform, we see that, for $\tau\to\infty$,

$$F(\tau) \to \frac{1}{\tau}\int d\omega\tilde{N}(\omega) = \frac{1}{\tau}N(0), \tag{82}$$

with correction terms starting with $-iN'(0)/\tau^2$. Thus, if $N(0)=0$, we have that F behaves like $1/\tau^2$. Going back to the solution (81), we see that it is only possible to let F go like $1/\tau$, which fixes the integration constant to be $C=i$. Then,

$$F(\tau) = \frac{2f}{\beta}\frac{ib}{1+ib\tau}. \tag{83}$$

We can now perform the Fourier transform (67) by means of Cauchy's theorem, and we obtain

$$N(x) = \frac{2f}{\beta}e^{-x/b}. \tag{84}$$

It is easily verified that this function satisfies the original integro-differential equation (54) without the diffusion term. The solution is identical to the one found in [27] by noticing that in the case of no diffusion b can be expressed in terms of the total "mass" $M=\int_0^\infty dx x N(x)$ from Eq. (53) as $b=\sqrt{\beta/(2f)M}$. Clearly, this solution does not satisfy $N(0)=0$. Instead there is a piling up at $x=0$ given by the ratio of fragmentation versus merging. The more fragmentation one has, the more piling up comes about for small x. Also, the more merging one has, the less piling up at small x. These results are of course physically reasonable.

IX. EFFECT OF DIFFUSION

If diffusion is included, it will have the profound effect that it is possible to enforce the boundary condition $N(0)=0$. We then have to consider the full Riccati equation (63). Unfortunately we have not been able to solve this equation exactly, in contrast to the no-diffusion case considered in the last section. Therefore we need to find an approximate solution valid in different τ ranges. In this connection it should be pointed out that if $F(\tau)$ is (i) analytic in the upper half plane and (ii) grows less than exponential on a large semicircle in the upper half plane, then there is only the trivial solution $N(x)=0$. This simply follows by the use of Eq. (67) by closing the contour in the upper half plane at no price, since there is an exponential damping from the factor $\exp(ix\tau)$ due to (ii). Application of Cauchy's theorem then gives the trivial result, since no singularities are included inside this contour, due to (i). Therefore, to have a nontrivial approximate solution at least one of the two conditions (i) and (ii) must be violated.

To see that the boundary condition $N(0)=0$ is possible when diffusion is included, we notice that for large τ the linear second-order equation (66) has the solution

$$u(\tau) \approx \text{const} \times \left(1 + \frac{i\beta}{2fx_0\tau}N'(0) + O(1/\tau^2)\right), \text{ i.e.,}$$

$$\ln u(\tau) \approx \text{const} + \frac{i\beta}{2fx_0\tau}N'(0) + O(1/\tau^2), \tag{85}$$

which comes as a cancellation of the diffusive terms $-i\tau^2u'(\tau)$ and $+(\beta/2fx_0)N'(0)$. Using Eq. (65) we have

$$N(0) = \frac{1}{2\pi i}\int_{-\infty}^{\infty} d\tau F(\tau) = \frac{2fx_0}{\beta}\frac{1}{2\pi i}\int_{-\infty}^{\infty} d\tau \frac{d}{d\tau}\ln u(\tau)$$

$$= \frac{2fx_0}{\beta}[\ln u(\tau)]_{-\infty}^{\infty} = 0. \tag{86}$$

It should be noticed that in the case of no diffusion the asymptotic behavior of $u(\tau)$ is different, $u(\tau) \approx \text{const} + O(\ln \tau)$.

We shall now show that if one has an approximate pole behavior of $F(\tau)$ this represents a saddle point in the Fourier integral (67). This is important, since we cannot directly use Cauchy's theorem to perform the integral if the solution is only approximate and dominates only near a pole τ_0. From the Fourier integral we see that there is a stationary phase (or saddle point) when

$$ix\tau - \ln(\tau - \tau_0) \tag{87}$$

is stationary, which happens for

$$ix - \frac{1}{\tau - \tau_0} = 0, \text{ i . e . , } \tau = \tau_0 + \frac{1}{ix}. \tag{88}$$

Also, the second derivative of the phase $-x^2/4$ is negative, so the saddle point is stable. The value of $N(x)$ in this saddle point is

$$N(x) \approx \text{const} \times \sum e^{i\tau_0 x}, \tag{89}$$

where we should sum over all relevant τ_0's subject to the condition that $N(x)$ be finite and positive.

We shall now investigate the possibility that there exists a pole for small values of τ. To this end we shall use that from Eq. (65) a pole in $F(\tau)$ can show up as a zero in the function $u(\tau)$, which satisfies the linear second-order equation (66). Let us tentatively assume that this pole occurs for small values of τ, so that we can expand

$$u(\tau) \approx 1 + c_1\tau + c_2\tau^2 + \cdots, \tag{90}$$

where the first constant is taken to be 1, since the overall scale of $u(\tau)$ is irrelevant for $F(\tau)$. From Eq. (66) we then obtain

$$u(\tau) \approx 1 + i\frac{b}{x_0}\tau + \frac{\beta}{2x_0 f}N'(0)\tau^2 + \cdots. \tag{91}$$

There is indeed a pole $u(\tau_0) \approx 0$,

$$\tau_0 = \frac{i}{\beta/(fx_0)N'(0)}[\sqrt{(b/x_0)^2 + 2\beta/(fx_0)N'(0)} - b/x_0], \tag{92}$$

where we took the root which leads to a finite result for $N(x)$ by use of Eq. (89). Using Eq. (53) this can be written

$$\tau_0 = \frac{i}{\langle x\rangle - b/x_0}\left(\sqrt{\frac{2\langle x\rangle}{b/x_0} - 1} - 1\right). \tag{93}$$

It is clear that this result is only valid provided $|\tau_0|$ is small, since otherwise more terms should be included in the expansion (90)

Now the question naturally appears as to whether there are other saddle points relevant when τ is large? In general, the saddle points are in the complex τ plane, as we saw in the pole case discussed above, where τ_0 is imaginary. In this connection we remind the reader that in the case of no merging, we obtained as a solution an oscillating integral (71), which could be turned into an integral (77) which is damped at large τ by deforming the contour. On the deformed contour the Fourier transform is thus small for large τ. Motivated by these considerations we ask if there exists an approximate solution of the Riccati equation (63) where F is small. In this case we can ignore the quadratic term, and the equation reduces to

$$-\frac{dF(\tau)}{d\tau} + \left(\frac{2}{\tau} + i\tau^2 + \frac{2ib}{x_0}\right)F(\tau) - N'(0) - 2i\frac{\tilde{\beta}}{\beta\tau} \approx 0. \tag{94}$$

We see that except for the term $(2ib/x_0)F(\tau)$ the equation is the same as the equation with no merging, Eq. (73), and the solution is the same as Eq. (74), except for a contribution $\exp(2ib/x_0\tau)$. Again there is a null function with respect to the Fourier integral (67), similar to the one that occurs in Eq. (74). Ignoring the null function we have

$$F(\tau) \approx \text{const} \times \tau^2 e^{(i/3)\tau^3 + (2ib/x_0)\tau}. \tag{95}$$

Along the contour forming angles $\pi/6$ and $5\pi/6$ with the real axis this function is small for large values of τ. The expression for $N(x)$ is then

$$N(x) \approx \text{const} \times \int_{-\infty}^{\infty} d\tau\tau^2 e^{(i/3)\tau^3 + (2ib/x_0)\tau + ix\tau}. \tag{96}$$

For large x this leads to a saddle point in the Fourier transform (67) well known from the theory of Airy functions. It occurs at $\tau = i\sqrt{x}$ and is stable,

$$N(x) \approx \text{const} \times x^{3/4} e^{(-2/3)x^{3/2} - (2b/x_0)x^{1/2}}. \tag{97}$$

To conclude this discussion, we see that there are in principle two saddle points (at least, there may be others that we have overlooked). The one given by the slope (93) always dominates, because it decays exponentially in contrast to Eq. (97). However, there may be a transitory region for large, but not too large x, where the behavior is given by Eq. (97), but for very large x the behavior is always dominated by the slope (93). If the slope (93) increases to around 1, expression (93) is no longer expected to be valid, since more terms would be needed in the expansion (90).

X. NUMERICAL RESULTS

The most direct way of validating the theoretical predictions presented in the preceding section is to integrate Eq. (51) numerically. Inevitably, a numerical approach implies that the domain of the function $N(x)$ will be restricted to a finite set of natural numbers $X = \{0, 1, \ldots, L\}$. Here, we must ensure that L is chosen sufficiently large to suppress finite-size effects and that X is sufficiently "dense" to give a proper

representation of the continuous function N. The second requirement is satisfied by rescaling the diffusion to fragmentation ratio so that $x_0^{-1}=(D/f)^{-1/3}\ll 1$. Consequently, L must be chosen such that $L/x_0\gg 1$. As we have seen, the other relevant length scale is set by the coagulation to fragmentation ratio $b=(\beta/2f)\int_0^\infty N(x)$. Since diffusion processes will always be dominating for small values of x, this length scale only plays a part in setting the upper limit—i.e., $L/b\gg 1$. The most important concern in choosing L comes from the problem of ensuring the mass conservation of Eq. (51), $\partial_t\int_0^\infty dxN(x,t)x=0$. The proper discretized version of the fragmentation and coagulation operators that entails mass conservation in the finite domain X reads

$$[\partial_t N]_{\text{frag}} \to [\partial_t \tilde{N}]_{\text{frag}} = -f(\tilde{x}-1)\tilde{N}(\tilde{x}) + 2f\sum_{\tilde{x}'=\tilde{x}+1}^{L}\tilde{N}(\tilde{x}') \tag{98}$$

and

$$[\partial_t N]_{\text{coag}} \to [\partial_t \tilde{N}]_{\text{coag}} = \beta/2\sum_{\tilde{x}'=0}^{\tilde{x}-1}\tilde{N}(\tilde{x}')\tilde{N}(\tilde{x}-\tilde{x}') - \beta\tilde{N}(\tilde{x})\sum_{\tilde{x}'=0}^{L-\tilde{x}}\tilde{N}(\tilde{x}'), \tag{99}$$

where $\tilde{N}$ represents the discretized function. The discrete Laplacian

$$\partial_x^2 N(x) \to \Delta^2\tilde{N}(\tilde{x}) = \begin{cases} \tilde{N}(1)-2\tilde{N}(0) & \text{for } \tilde{x}=0, \\ \tilde{N}(\tilde{x}+1)+\tilde{N}(\tilde{x}-1)-2\tilde{N}(\tilde{x}) & \text{for } 0<\tilde{x}<L, \\ \tilde{N}(L-1)-2\tilde{N}(L) & \text{for } \tilde{x}=L, \end{cases} \tag{100}$$

however, will always lead to a net loss of the total mass, since

$$\sum_{\tilde{x}=0}^{L}\tilde{x}\Delta^2\tilde{N}(\tilde{x}) = -(L+1)\tilde{N}(L). \tag{101}$$

Here, we take the simplest approach of setting L so that the relative loss of mass will be small in each time step—i.e., $L\tilde{N}(L)\ll\Sigma_{\tilde{x}=0}^{L}\tilde{x}\tilde{N}(\tilde{x})$. Since for all parameters of b/x_0 we expect the distributions to display an exponential decay (at least), the mass loss will automatically be small when $L/x_0\gg 1$ and $L/b\gg 1$. In the following we present results using $x_0\approx 50$ and $L=1000$ for values of $b/x_0\leqslant 2$ and $L=10\,000$ for $b/x_0>2$. The discretized equation

$$\partial_t\tilde{N}(\tilde{x}) = \Delta^2\tilde{N}(\tilde{x}) + [\partial_t\tilde{N}]_{\text{frag}} + [\partial_t\tilde{N}]_{\text{coag}} \tag{102}$$

is solved using a fourth-order Runge-Kutta integration scheme with variable time step [30,31]. Convergence is obtained by requiring that the relative change $\Delta\mathcal{N}$ of the total counts, $\mathcal{N}=\Sigma_{x=0}^{L}\tilde{N}(x)$, during a time interval of $\Delta t=1$ satisfy $\Delta\mathcal{N}/\mathcal{N}<10^{-6}$. For all calculations the time-integrated mass loss is less than 0.1% compared to the mass of the initial distribution.

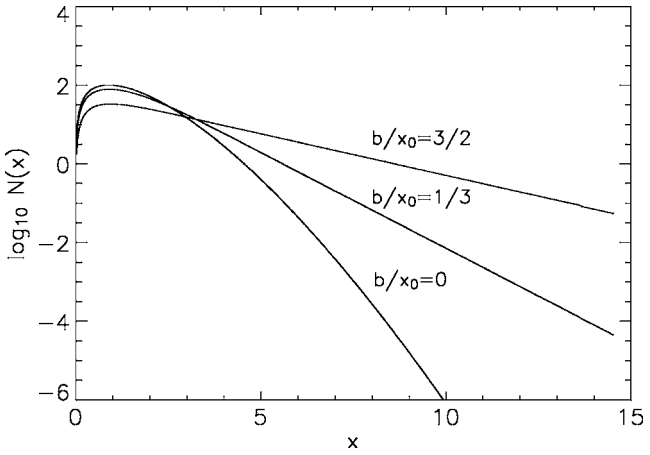

FIG. 3. The numerical steady-state distributions $N(x)$ as a function of x (both quantities dimensionless) for different coagulation-to-fragmentation ratios b/x_0.

In Fig. 3 we show $N(x)=\tilde{N}(\tilde{x})$ as a function of $x=\tilde{x}/x_0$ for different values of b/x_0. For small values of b/x_0, one indeed observes a crossover from the functional form, Eq. (97), at intermediate values of x to a pure exponential for large values of x. At larger values of b/x_0, only a single-exponential form is observed for $x>1$.

In Fig. 4 we show the slope $\text{Im}(\tau_0)$ of the exponential tail of the distributions as function of b/x_0. The full curve is expression (93), whereas the square diamonds are the slopes obtained from an exponential fit to the tail of the numerical solutions for different values of b/x_0. For $\text{Im}(\tau_0)<1$, which corresponds to values where the coagulation to fragmentation ratio is the dominant length scale, $b>x_0$, we find perfect agreement between the theoretical predictions and the numerical results.

We shall now use a simple one-dimensional lattice model as an alternative approach to put the aforementioned theory to a test. We pick a finite lattice of length L and impose

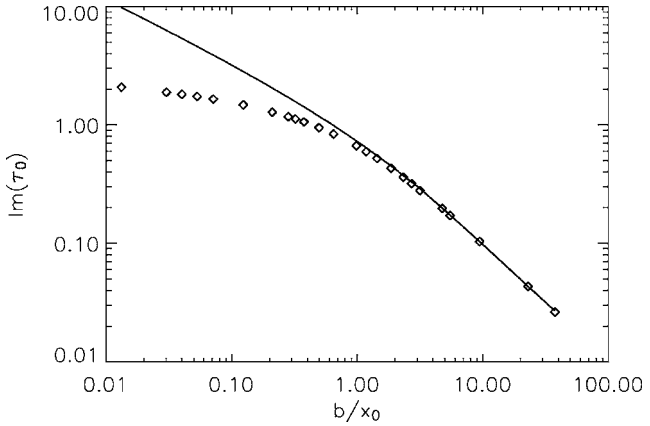

FIG. 4. The slope $\text{Im}(\tau_0)$ (dimensionless) of the exponential tail of $N(x)$ as a function of b/x_0. The solid line is the theoretical prediction, Eq. (93), and the square diamonds are the numerical results. One observes a perfect agreement for all $\text{Im}(\tau_0)<1$.

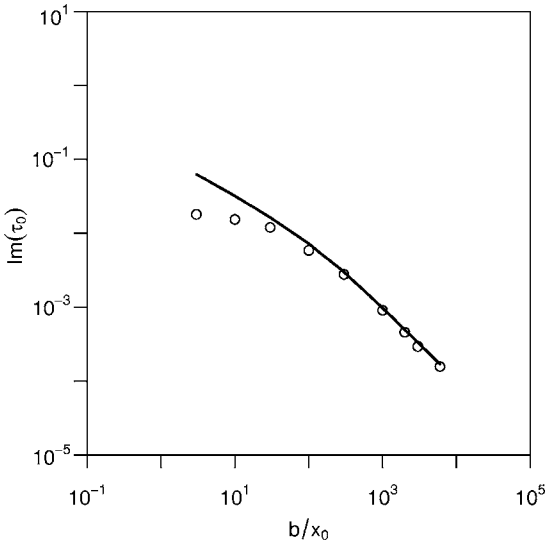

FIG. 5. Lattice simulation data of Im τ_0 as a function of $b=\tilde{\beta}/f$. The line represents the analytical expression of Im τ_0.

periodic boundary conditions. On the lattice we initially distribute a set of $\mathcal{N}$ clusters of sizes $\{\ell_i\}_{i=1}^{\mathcal{N}}$ and with a total mass chosen to fit the lattice length, $\sum_i \ell_i = L$. We define the cluster boundaries by a new set $\{x_i\}_{i=1}^{\mathcal{N}}$ such that $\ell_i = x_i - x_{i-1}$ (with $x_0 = x_N - L$). The diffusion process of Eq. (51) corresponds in the lattice model to a random walk of the boundaries, and therefore in each time step we update the boundary positions according to $x_i(t+1) = x_i(t) \pm 1$. Here the lattice spacing and time steps, as well as the diffusion constant, are chosen to be unity. A fragmentation event is simulated by introducing a new random walker or boundary $\tilde{x}$ on the lattice. The position of $\tilde{x}$ is picked uniformly among the $L-\mathcal{N}$ available lattice sites. Effectively, we therefore get a constant fragmentation rate given by $f=n/L$, where n is the number of new boundaries introduced in each time step. Finally, the coagulation process is similar to the removal of boundaries. In each time step a random walker is removed with a probability γ. Note that γ is equivalent to the rate $\tilde{\beta}=\beta\mathcal{N}$ introduced in Eq. (52). The equivalence follows by comparing the number of events where a cluster of size x coagulates with a cluster of size y. In the lattice model, the number of events in a unit time is $\mathcal{N}\gamma[N(x)/\mathcal{N}]N(y)/\mathcal{N}$, which should be compared with the corresponding number in Eq. (51), and thus we get $\gamma/\mathcal{N}=\beta$. In order to minimize the effect of the underlying lattice it is important to keep the total mass or lattice length L of the system much larger than any other scale in the system—i.e., $L \gg (D/f)^{1/3}$ and $L \gg \tilde{\beta}/f$. Figure 5 presents estimates of Eq. (93) based on the lattice model with a lattice size $L=10^7$. We collect the simulation data in a histogram with a unit bin size and then fit the exponent of the tail. The maximum count in any bin is for reasonable amounts of computer time limited above by 10^8; thus, we have a bound on the maximum exponent that is possible to estimate and we have an explanation why the lattice simulations provide poor estimates in Fig. 5 for low values of b.

Compared to the direct numerical integration there are both advantages and disadvantages. First of all the lattice model is extremely simple from a computational point of view and does by construction conserve the total mass. Moreover, the model reproduces to high accuracy, using little computer time, the theoretical predictions for large values of b/x_0, which is in contrast to the larger computational power needed in the direct numerical integration. Note that in the lattice model there is a weak size correlation between neighboring clusters. The diffusion makes some clusters large at the cost of the surrounding ones. The correlation is not present in the mean-field equation (51), and it may be avoided on the lattice by shuffling in each time step the clusters. By implementing this shuffling in the numerical routine, it however turns out that the correlation has negligible or no effect on the cluster size distribution.

XI. CONCLUSION

In this paper, we have introduced a model which includes the three fundamental physical processes: diffusion, fragmentation, and coagulation. The model is formulated as a dynamical equation in terms of the distribution $N(x,t)$ of fragment sizes x. The main results of the paper are the following: In the case of no coagulation term, we obtain an exact solution for the distribution of the Bessel type $\exp(-\frac{2}{3}x^{3/2})$. When the coagulation terms is added, we show that the nonlinear equation can be mapped exactly onto a Riccati equation. From solution of this equation we obtain that the distribution now turns into a pure exponential for large x. When the coagulation process is small as compared to the fragmentation process, we identify directly that the distribution $N(x)$ behaves as the Bessel function for small x after which it crosses over to an exponential at a specific value of x.

We believe that our proposed model is relevant in many physical situations, such as for solutions of macromolecules like polymers, proteins, and micelles. In fact, from measured distributions of fragment sizes we suggest that one might be able to identify how important the coagulation process is compared to the fragmentation process. We are in the process of collecting experimental data for such investigations.

[1] M. von Smoluchowski, Phys. Z. **17**, 557 (1919); **17**, 585 (1916).
[2] M. von Smoluchowski, Z. Phys. Chem., Stoechiom. Verwandtschaftsl. **92**, 129 (1917).
[3] F. Leyvraz, Phys. Rep. **383**, 95 (2003).
[4] Z. A. Melzak, Trans. Am. Math. Soc. **85** 547 (1957).
[5] R. M. Ziff, J. Stat. Phys. **23**, 241 (1980).
[6] S. K. Frielander. *Smoke, Dust and Haze: Fundamentals of Aerosol Dynamics* (Wiley, New York, 1977).
[7] J. Silk and S. D. White, Astrophys. J., Lett. Ed. **223**, L59

(1978).
[8] A. Okubo, Adv. Biophys. **22**, 1 (1986).
[9] S. Gueron and S. A. Levin, Math. Biosci. **128**, 243 (1995).
[10] R. L. Drake, in *Topics in Current Aerosol Research*, edited by G. M. Hidy and J. R. Brock (Pergamon, Oxford, 1972), Pt. 2, pp. 201–376.
[11] P. Laurençcot and S. Mischler, in *Modeling and Computational Methods for Kinetic Equations*, edited by Pierre Degond, Lorenzo Pareschi, and Giovanni Russo, Modeling and Simulation in Science, Engineering and Technology (MSSET) Series (Birkhauser, 2004).
[12] J. Ferkinghoff-Borg, M. H. Jensen, J. Mathiesen, P. Olesen, and K. Sneppen, Phys. Rev. Lett. **91**, 266103 (2003).
[13] J. Mathiesen, J. Ferkinghoff-Borg, M. H. Jensen, M. Levinsen, P. Olesen, D. Dahl-Jensen, and A. Svenson, J. Glaciol. **50**, 325 (2004).
[14] H. Amann, Arch. Ration. Mech. Anal. **151**, 339 (2000); H. Amann and F. Weber, Adv. Math. Sci. Appl. **11**, 227 (2001); P. Laurençcot and S. Mischler, Arch. Ration. Mech. Anal. **162**, 45 (2002).
[15] M. Hillert, Acta Metall. **13**, 227 (1965).
[16] N. P. Louat, Acta Metall. **22**, 721 (1974).
[17] R. B. Alley, J. H. Perepezko, and C. R. Bentley, J. Glaciol. **32**, 415 (1986).
[18] R. B. Alley, J. H. Perepezko, and C. R. Bentley, J. Glaciol. **32**, 425 (1986).
[19] B. J. McCoy, J. Colloid Interface Sci. **240**, 139 (2001).
[20] H. Flyvbjerg, T. E. Holy, and S. Leibler, Phys. Rev. Lett. **73**, 2372 (1994).
[21] H. Flyvbjerg, T. E. Holy, and S. Leibler, Phys. Rev. E **54**, 5538 (1996).
[22] B. H. Zimm and J. K. Bragg, J. Chem. Phys. **31**, 526 (1959).
[23] P. Laurençcot, Banach Cent Publ. **66**, 211 (2004).
[24] M. H. Ernst and G. Szamel, J. Phys. A **26**, 6085 (1993).
[25] E. D. McGrady and R. M. Ziff, Phys. Rev. Lett. **58**, 892 (1987).
[26] M. Aizenman and T. A. Bak, Commun. Math. Phys. **65**, 203 (1979).
[27] I. W. Stewart and P. B. Dubovskii, Math. Methods Appl. Sci. **19**, 171 (1996).
[28] G. N. Watson, *A Treatise on the Theory of Bessel Functions* (Cambridge University Press, Cambridge, England, 1944).
[29] N. Nielsen, *Die Zylinderfunktionen und ihre Anwendungen* (Teubner Verlag, Leipzig, 1904).
[30] Note that Eq. (51) can also be rewritten as a second-order differential equation in terms of the cumulative mass distribution. This rewriting has been used in A. A. Lushnikov and M. Kulmala, Phys. Rev. E **65**, 041604 (2002).
[31] W. H. Press, S. A. Teukolsky, W. T. Vetterling and B. P. Flannery, *Numerical Recipes in C*, 2nd ed. (Cambridge University Press, Cambridge, England, 1992).